

A Thermal Resistance Capacity Evaluation Method of Geothermal Energy: A Case Study in the Chingshui Geothermal Field, Ilan, Northeastern Taiwan

David Ta-Wei Lin* and Kanjanaporn Chaichana**

Keywords: Capacity evaluation; Thermal resistance; Brinkman model

ABSTRACT

Nowadays, there is no effective method to evaluate the efficiency of geothermal power plant but capacity test of in-situ. This is due to the poor-known thermal-fluid information about the reservoir. This study proposes an innovative Capacity Evaluation method based on the thermal resistance of well. The capacity evaluation model of geothermal well consists of the Brinkman model conjugated with heat transfer model and the pipe flow model. This capacity evaluation model is validated with the capacity test of the geothermal well of IC 09 & 13 in Chingshui, Taiwan. The thermal resistance of these wells can be obtained through the in-situ data of the geometry, well temperature, and mass flow rate. The capacity of geothermal can be optimized as the reasonable capacity evaluation model is built. In the thermal resistance view, the key technology will be proposed for building the reliable and convenient evaluated model of geothermal capacity.

INTRODUCTION

Comparing with the solar energy and wind energy, geothermal energy is a stable and base load power (Li, 2015). The technology and theory of geothermal system achieves the independent engineering field and commercial scale gradually (Fridleifsson, 2001). The production of geothermal energy can be improved by the technology of exploitation, the heat

exchange skills, the knowledge of geothermal information, as the geothermal power development in recent year. Geothermal development needs to find the suitable site, include geology, thermal dynamics, mechanical engineering and electric engineering. Scientists propose lots of suggestions for evaluating the geothermal potential and building the global phenomena of geothermal field. However, the capacity test still should be processed as the evaluating the enthalpy of the working fluid. It is an important step to evaluate the economic cost of geothermal power plant.

Besides the capacity test, the evaluated model is improved for the complex phenomena and pre-selected plan. Pruess built the numerical model TOUGH for the multiphase flow in permeable media in 2004 (Pruess, 2004). The THM model is developed and been used to investigate the EGS with fracture network by anisotropic model (Liao et al., 2020). Many phenomena and availabilities of geothermal energy are investigated such as thermal breakthrough prediction (Liu et al., 2020), well spacing problem (Chen et al., 2021), the reutilization of oil or gas well (Harris et al., 2021), Lots of phenomena are still difficult to clarify such as chemical reactions in the reservoir such as the fluid-rock interaction (Xu, et al. 2006), the effects of brine (Xu et al., 2009) which result in the temperature contour of the reservoir. The numerical model is improved and innovated for involving more geologic and heat mass transfer conditions. The EGS (enhance geothermal system) with dual porous medium and fracture are modelled by THM model for the related complex reservoir (Ren et al., 2020). Wang et al. propose the heat extraction of multilateral -well coaxial closed-loop geothermal system based on the COMSOL software (Wang et al., 2021).

Nowadays, there is no effective method to evaluate the efficiency of geothermal power plant but capacity test. This is due to the poor-known thermal-fluid information about the reservoir. The uncertainty of geothermal power is hardly controlled such as the number of preferential flow pathways (Patterson et al., 2020).

However, the above approaches have some

*Paper Received October, 2022. Revised November, 2022.
Accepted December, 2022. Author for Correspondence:
David T.W. Lin.*

* *Professor, Institute of Mechatronic System Engineering,
National University of Tainan, Tainan 70005, Taiwan*

** *Institute of Mechatronic System Engineering, National
University of Tainan, Tainan 70005, Taiwan*

limits in this application. The important limitation is hardly to handle the whole mechanics in the reservoir. Actually, the total enthalpy from the well is the key point for the electric potential. In this view, this study proposes a thermal resistance concept to find the optimal operated parameters for extracting heat. Therefore, the relationship between the well capacity test and total enthalpy could be decided based on a conceptual. It will provide a global view to find the potential but the local phenomena. It is the purpose of this study to propose a capacity evaluation model. This model will reduce the cost of capacity test and benefit to the design of geothermal power plant.

The reservoir of Brinkman model conjugated with heat transfer model is proposed by our team and fitted the thermal dispersion by experiment in two kinds of mass flow rate under various pressure. Based on the fitted reservoir model, the optimal results by the optimal simplified conjugated gradient method (SCGM) are presented.

CAPACITY EVALUATION MODEL

A capacity evaluation model is proposed firstly. That is, the thermal resistance of the well is proposed to represent the heat transfer feature of the well. The temperature profile of the well can be obtained from the capacity test of in-situ and the well thermal hydraulic (TH) model. The thermal resistance of this well can be calculated from the heat dissipation and temperature difference between well and environment. This well TH model consists of the Brinkman model conjugated with porous heat transfer model simulated as the reservoir and the pipe flow model as the well. The thermal dispersion of this numerical model will be obtain from the fitting of the thermal dispersion experimental results. In addition, the optimization of this capacity evaluation model will process to obtain the optimal operated condition for the maximum capacity. The schematic diagram and process of capacity evaluation model are shown in Figs 1 & 2.

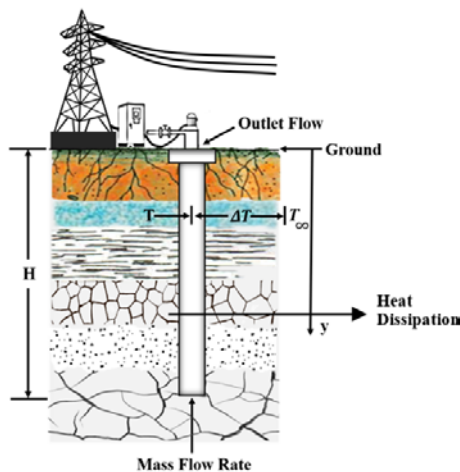


Fig. 1 The schematic diagram of capacity evaluation model.

The geometry and boundary of this model are built based on the in-situ capacity test of single well No. IC09 & IC 13 in Chingshui. The thermal resistance of geothermal well of in-situ can be obtained.

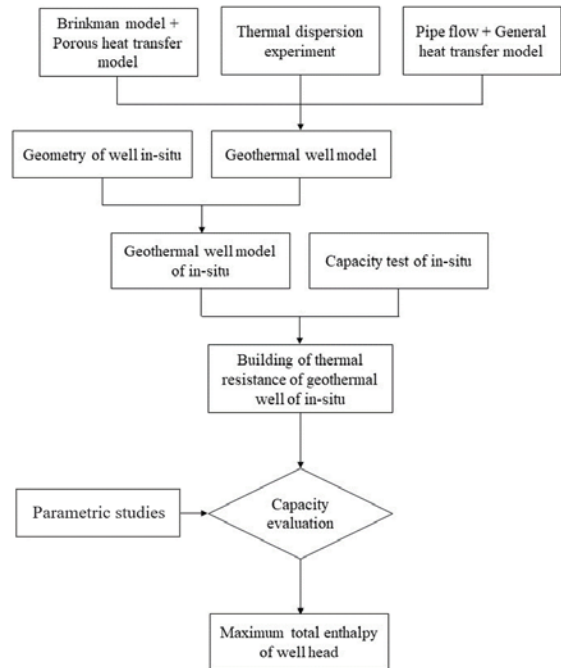


Fig. 2 The architecture of capacity evaluation model.

The detailed illustrations of this architecture of capacity evaluation are exhibited as below. First, the well porous TH model is built based on the Brinkman model conjugated with heat transfer model. The thermal dispersion length is obtained from the fitting process of thermal dispersion experiment. Here, the governing equations of the porous model are described as below:

Continuity equation is:

$$\frac{\partial}{\partial t}(\varepsilon\rho) + \nabla \cdot (\rho u) = Q_{br} \quad (1)$$

Momentum equation is:

$$\frac{\rho}{\varepsilon} \left(\frac{\partial u}{\partial t} + (u \cdot \nabla) \frac{u}{\varepsilon} \right) = -\nabla p + \nabla \cdot \left[\frac{1}{\varepsilon} \left\{ \mu(\nabla u + (\nabla u)^T) - \frac{2}{3} \mu(\nabla \cdot u)I \right\} \right] - \left(\frac{\mu}{\kappa} + \frac{Q_{br}}{\varepsilon^2} \right) u + F \quad (2)$$

where μ is viscosity; u is velocity; ρ is fluid density; p is pressure and F is forced term; ε is porosity; κ is permeability and Q_{br} is mass force.

The Fourier's law of porous medium is described as below:

$$\frac{\partial}{\partial t} [(1 - \varepsilon)\rho_p C_{p,p} T_p] - (1 - \varepsilon)\nabla \cdot (k_p \nabla T_p) = 0 \quad (3)$$

Energy balance equation is:

$$\frac{\partial}{\partial t} [\varepsilon\rho_f C_{p,f} T_f] + \nabla \cdot (\rho_f C_{p,f} D T_f) - \varepsilon\nabla \cdot (k_f \nabla T_f) = 0 \quad (4)$$

where T is temperature; C_p is specific heat; k is thermal conductivity, D is Darcy flow and the

subscript label f means fluid and pis media.

Second, the well part is based on the pipe flow and general heat transfer model. The governing equations (non-porous medium) are described as below. Continuity equation is:

$$\frac{\partial \rho}{\partial t} + \nabla \cdot (\rho u) = 0 \quad (5)$$

Momentum equation is:

$$\rho \frac{\partial u}{\partial t} + \rho(u \cdot \nabla)u = \nabla \cdot [-pI + \mu(\nabla u + (\nabla u)^T) - \frac{2}{3}\mu(\nabla \cdot u)I] + F \quad (6)$$

Energy balance equation is described as below:

$$\frac{\partial}{\partial t} [\rho C_p T] + \nabla \cdot (\rho C_p u T) - \nabla \cdot (k \nabla T) = 0 \quad (7)$$

The schematic diagram of this model is shown in Fig 3. The heat and mass transfer analysis are built by this model.

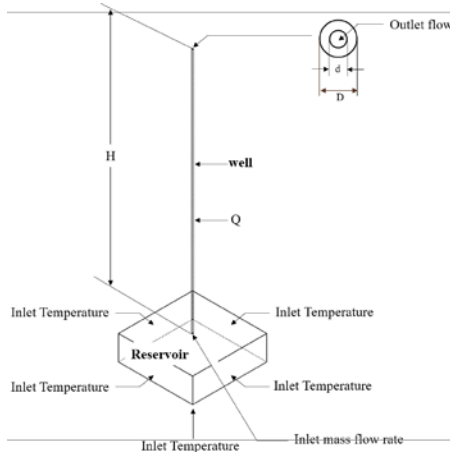


Fig. 3 The schematic diagram of well porous TH model.

Thermal dispersion length

The thermal dispersion of this well porous TH model is adjusted from the fitting process of the results of thermal dispersion experiment.

A thermal dispersion experiment (working fluid is water) is set under the similar conditions of this geothermal well. The experimental process and installation are described in the previous research (working fluid is supercritical CO₂) of our team (Lin et al., 2019). Through this process, Q (heat extraction) and ΔT (temperature difference between the exit and inlet of test section) of numerical model are close to the results of experiment as the thermal dispersion length adjusting. From the view of thermal resistance, the model and experiment are similar under the same geometry and thermal-fluid conditions. The model with two kinds of porosity (particle size is 1.54 mm and 2.03 mm), and four kinds of inlet mass flow rates (0.00033 kg/s, 0.00066 kg/s and 0.00099 kg/s and 0.00132 kg/s) are processed. Fig. 4 presents the fitting results of this porous heat transfer model. Fig. 4(a) and (b) is the fitting result of the temperature difference and heat extraction.

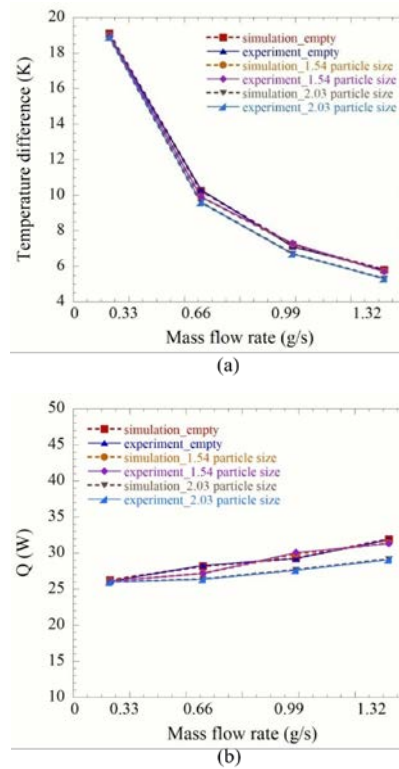


Fig. 4 The fitted results of simulation compared with the experiment (a) temperature difference (b) the heat extraction through the test tube.

Through this fitting process, the heat extraction and temperature difference of the simulation will be approached to the ones of experiment. The error of heat extraction between the simulation and experiment is 1.3 % and 1.1 % in particle size is 1.54 mm and 2.03 mm, respectively.

Porous TH model of geothermal well No. IC09 & 13

The location of IC09 & IC13, Chingshui, ILan, Taiwan is shown in Fig 5 and the results of capacity test are listed in Table 1 & 2.



Fig. 5 The location of IC09 & IC13, Chingshui, ILan, Taiwan.

Table 1 Capacity test and Geometry of IC09, Chingshui

	Depth (m)	Diameter (Test tube) (inch)	Temp. (Bottom of well) (°C)	Temp. (Outlet) (°C)	Pressure (Outlet) (Bar)	\dot{m} (ton/hr)	\dot{m}_{vap} (ton/hr)	\dot{m}_{liq} (ton/hr)	Date
Case1	2086	1.5	200	168.7	9.2	19.5	3.5	16	2008/4/29-30
Case2	2086	2	200	160.4	7	27.2	4.5	22.7	2008/4/28-29
Case3	2086	2.5	200	151.2	5.3	31.9	6	25.9	2008/4/27-28
Case4	2086	3	200	146.1	4	34.2	8	26.2	2008/4/30-5/7

Table 2 Capacity test and Geometry of IC13, Chingshui

	Depth (m)	Diameter (Test tube) (inch)	Temp. (Bottom of well) (°C)	Temp. (Outlet) (°C)	Pressure (Outlet) (Bar)	\dot{m} (ton/hr)	\dot{m}_{vap} (ton/hr)	\dot{m}_{liq} (ton/hr)	Date
Case1	1275.02	1.38(35mm)	>217.1	180	8	25.5	6.8	18.7	2017/10/26
Case2	1275.02	1.5	>217.1	185	14.2	31.2	5.2	26	2009/7/8-9
Case3	1275.02	2	>217.1	173.7	9.3	34.7	8.7	26	2009/7/9-10
Case4	1275.02	2.5	>217.1	164.3	7.3	39.7	12.3	27.4	2009/7/10-11

The depth of well, the temperature of well bottom, the flow rate of steam, water and temperature of wellhead are listed in Table 1 & 2. Based on the fitted porous TH model and the capacity test of IC09 & IC13, Chingshui, Taiwan. Four kinds of capacity test are discussed to obtain the thermal resistance of IC09 & IC13, respectively.

The optimization of heat extraction under the varied test tube and mass flow rate can be obtained as the fitted simulated model is built. The numerical design approach is developed by combining a direct problem solver, COMSOL code (COMSOL, 2019), with an optimal method (the simplified conjugate gradient method, SCGM). The COMSOL package is used as the subroutine to solve the temperature profiles associated with mass flow rate of the well in the different test tube during the iterative optimal process.

The heat extraction of the geothermal well is chosen be the objective function, J , of this study, and the maximum objective function will be approached through the optimization.

$$J = \dot{m}h \quad (8)$$

here, h is the enthalpy of working fluid at the status of

wellhead.

RESULTS AND DISCUSSION

Thermal Resistance of IC09 & IC13

The thermal resistance of the well can be represented the characteristics of the geothermal well. The thermal resistance of this well can be calculated from the heat dissipation and temperature difference between well and environment (rock matrix) as Fig 1. The first, the heat dissipation of each case is obtained from a fitting of the capacity test of geothermal well in-situ (Table 1 and 2). The fitted results of IC09 and IC13 are shown in Table 3 and 4. The temperature profiles of the numerical model on IC09 & IC13 based on four kinds of capacity test are obtained and shown in Fig 8. Fig. 6(a) shows the temperature profile of IC09 as the test tube is 1.5 inch, 2 inch, 2.5 inch and 3 inch, separately. Fig 6(b) shows the temperature profile of IC13 as the test is 1.38 inch (35mm), 1.5 inch, 2 inch and 2.5 inch, separately. Along the well, the temperature decreasing from the bottom to the head is faster as the diameter of test tube increases.

Table 3 The heat dissipation of IC09, Chingshui

Diameter (Test tube) (inch)	Temp. (Bottom of well) (°C)	Temp. (Outlet) (°C)	Heat dissipation (kW)
1.5	200	168.7	732.85
2	200	160.4	1268.37
2.5	200	151.2	1779.11
3	200	146.1	2030.51

Table 4 The heat dissipation of IC13, Chingshui

Diameter (Test tube) (inch)	Temp. (Bottom of well) (°C)	Temp. (Outlet) (°C)	Heat dissipation (kW)
1.38(35mm)	>217.1	180	897.05
1.5	>217.1	185	1032.95
2	>217.1	173.7	1643.01
2.5	>217.1	164.3	2126.80

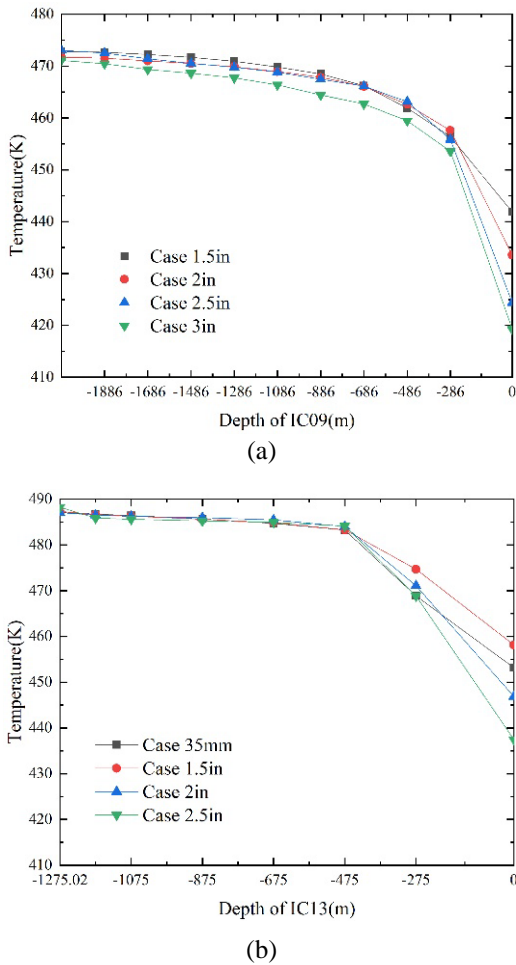


Fig. 6 The temperature profile of (a) IC09 (b) IC13 with difference capacity test.

The heat dissipation of IC09 and IC13 is shown in Fig 7, listed in Table 3 &4 in detail. As a whole, the heat dissipation increases as the diameter of test tube. The heat dissipation of case 1.38inch (35 mm) of IC13 is smaller about 10 % than the one of case 1.5 inch. It proves that the conditions of this case in 2009 is similar with the conditions in 2017.

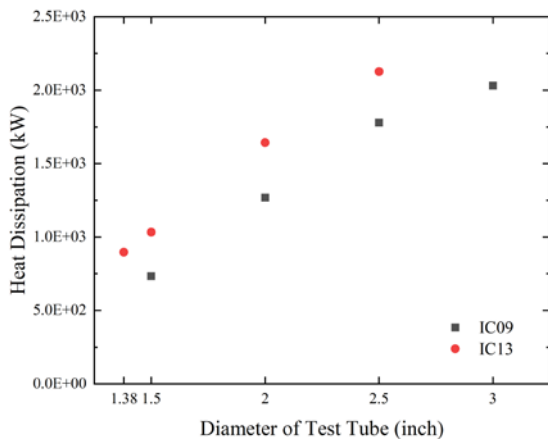


Fig. 7 The heat dissipation of IC09&IC13 with difference capacity test tube.

Next, the thermal resistance will be derived.

$$R_{th} = \frac{\Delta T}{\text{heat loss}} \quad (9)$$

here, ΔT is $\frac{1}{H} \int_{ground}^{bottom} T_{well} - T_{environment} dy$, it means the difference of the average temperature of well and environment.

The results of thermal resistance of IC09 and IC13 with the different test tube are shown in Fig 8, and listed in Table 5, separately. The thermal resistance decreases as the test tube increases for the reason of larger flow. Therefore, the thermal resistance can be an index to derive the geothermal capacity (heat extraction) with the different mass flow rate. The heat extraction with the different test tube is shown in Fig 9. Throughout the Fig 9, the heat extraction increases linearly when the test tube increases. In addition, for IC13, the heat extraction of the capacity test of 1.38in (35 mm) in 2017 and 1.5 in (about 38.1 mm) in 2009 is 10.5 MW and 11.3 MW. The results are almost linear exhibited even the test date of both of cases is 8 years away. From these results of in-situ capacity test of IC09 & IC13 in Chingshui, the variation of in-situ data over the past decade is very insignificant. We can conclude that the reference of geological in the decades is still meaningful in geothermal research.

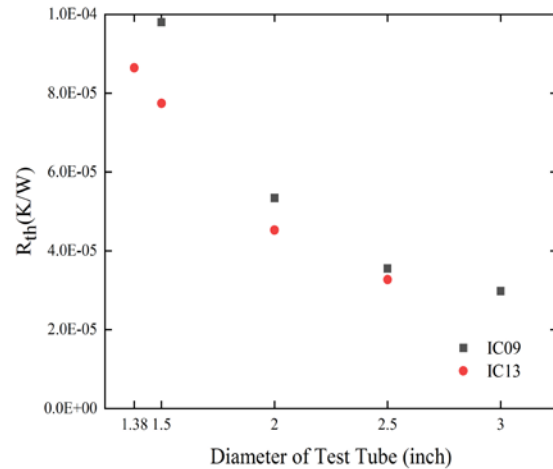


Fig. 8 The thermal resistance of IC09&IC13 with different capacity test tube.

Table 5 The thermal resistance with different capacity test tube in IC09 & IC13

	IC09		IC13	
	Diameter (Test tube)	Rth (K/W)	Diameter (Test tube)	Rth (K/W)
Case1	1.5 in	9.8E-5	35 mm	8.64E-5
Case2	2 in	5.34E-5	1.5 in	7.74E-5
Case3	2.5 in	3.55E-5	2 in	4.53E-5
Case4	3 in	2.98E-5	2.5 in	3.27E-5

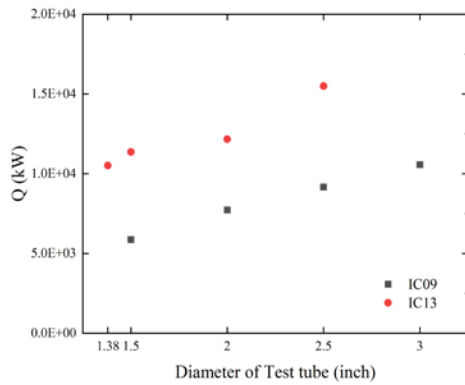


Fig. 9 The heat extraction of IC09&IC13 with difference capacity test tube.

Optimization

In general, the geothermal potential will be extracted as more as possible. Therefore, the geothermal flow will be induced by the pump. This study proves that the maximum geothermal potential exists even the geothermal flow keeps increasing. Through the optimization, the iteration of wellhead temperature of IC09 & IC13 with the mass flow rate of the geothermal flow under different test tube are shown in Fig 10. We can observe that the temperature of wellhead increases as the mass flow rate increases, therefore, the temperature difference decreases. It exhibits that the heat extraction will decrease as the geothermal flow increases. In IC09 & IC13, the temperature of wellhead increases slowly as the geothermal flow is greater than 15 kg/s and 25 kg/s, separately.

Fig. 10 The temperature (Thead) profile with the outlet mass flow rate (a) IC09 (b) IC13

We can conclude the optimized specific heat extraction will be obtained, if the pumping cost for increasing the mass flow rate is considered. Throughout Fig. 11, we observe that the increasing of specific heat extraction is moderate as the geothermal flow greater than 15 kg/s. The values of specific heat extraction at 5, 9, 11, 13, 15, 17, 19, 25, 40 kg/s of IC09 & IC13 are listed in Table 6. In table 6, the increasing rate of specific heat extraction of IC09 with 3 in test tube is 15 %, 4.2 %, 2 %, 0.64 % as the geothermal flow increases from 5 kg/s to 15 kg/s, 15-25 kg/s, 25-35 kg/s and 35-40 kg/s, separately. It indicates that it is invaluable to induce the geothermal flow as the increasing of specific heat extraction is not enough to make up the increasing of pump cost.

Table 6 The specific heat extraction (q) with different geothermal flow in IC09 & IC13

IC09		IC13			
Test tube	Mass flow rate(kg/s)	q (kW/kg)	Test tube	Mass flow rate (kg/s)	q (kW/kg)
3 inch	5	1016.5	5	5	1284.70
	10	1132.2	10	10	1397.15
	15	1169.50	2.5 inch	15	1432.60
	20	1193.98	20	20	1455.73
	25	1218.2	25	25	1478.40
	35	1242.2	35	35	1500.75

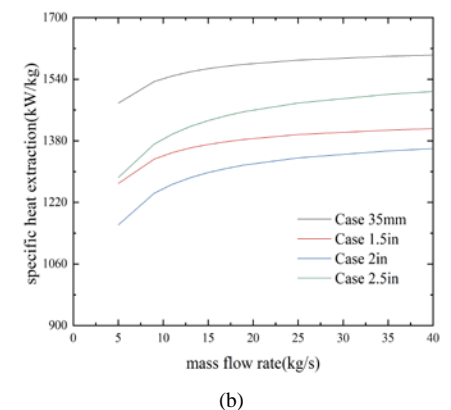
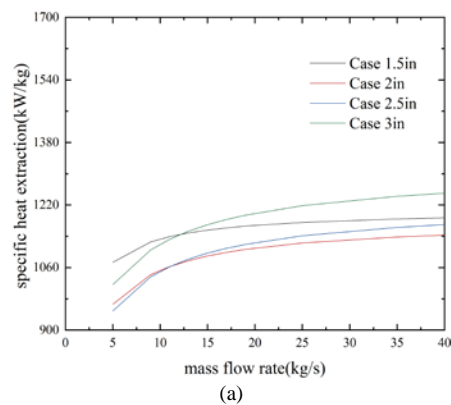
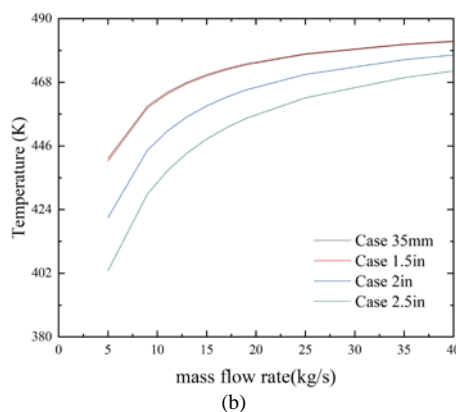
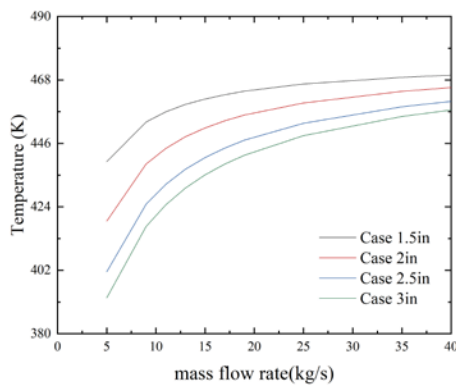


Fig. 11 The optimization of the specific heat extraction of (a) IC09 (b) IC13

CONCLUSIONS

An innovative capacity evaluation model is proposed and done based on the geothermal well IC09 & IC13, Chingshui, Taiwan in this study. The thermal resistance can be represented the characteristics of the geothermal well. Based on the results of thermal resistance, the specific heat extraction with different geothermal flow can be obtained. The limited specific heat extraction is observed with different geothermal flow and test tube in IC09 & IC13. This study proves that we can derive the maximum geothermal flow and potential based on few capacity test.

NOMENCLATURE

C_p	=specific heat (J/KgK)	ρ	=fluid density(Kg/m ³)
$(\rho C_p)_{\text{eff}}$	=effective volumetric capacity (J/m ³ K)	μ	=viscosity (Pa · s)
k	=thermal conductivity (W/mK)	ε	= porosity
k_{eff}	=effective volumetric thermal conductivity(W/mK)	ε_p	=volumetric fraction of the solid
F	=forced term (N)	κ	=permeability (m ²)
p	=pressure (pa)	λ_{lo}	=longitudinal dispersivity (m)
T	=temperature (K)	λ_{tr}	=transverse dispersivity (m)
u	=velocity (m/s)	Q_{br}	=mass force (N)

ACKNOWLEDGMENT

This work is supported by Ministry of Science and Technology, Republic of China (Taiwan) under grant MOST 110-2221-E-024 -010 and MOST 111-2221-E-024-008.

REFERENCES

Chen, S.Y., Hsieh, B.Z., Hsu, K.C., Chang, Y.F., Liu, J.W., Fan, K.C., Chiang, L.W., Han, Y.L., “Well spacing of doublet at the Huangtsuishan geothermal site, Taiwan,”; *Geothermics*, Vol. 89:101968(2021).

COMSOL Multiphysics version 5.5, November 14,

2019.

Fridleifsson, I.B., “Geothermal energy for the benefit of the people,”; *Renew. Sustain. Energy Rev.*, Vol. 5, pp.299-312(2001).

Harris, B.E., Lightsone, M.F., Reitsma, S., “A numerical investigation into the use of directionally drilled well for the extraction of geothermal energy from abandoned oil and gas wells,”; *Geothermics*, Vol. 90:101994(2021).

Li, K., Bian, H., Liu, C., Zhang, D., Yang, Y., “Comparison of geothermal with solar and wind power generation systems,”; *Renew. Sustain. Energy Rev.*, Vol. 42, pp. 1464-1474(2015).

Liao, J., Hou, Z., Haris, M., Tao, Y., Xie, Y., Yue, Y., “Numerical evaluation of hot dry rock reservoir through stimulation and heat extraction using a three-dimensional anisotropic coupled THM model,”; *Geothermics*, Vol. 83:101729(2020).

Lin, D.T.W., Hsieh, J.C., Shih, B.Y., “The optimization of geothermal extraction based on supercritical CO₂ porous heat transfer model,”; *Renew. Energy*, Vol. 143, pp. 1162-1171(2019).

Liu, G., Wang, G., Zhao, Z., Ma, F., “A new well pattern of cluster layout for deep geothermal reservoirs: Case study from the Dezhou geothermal field, China,”; *Renew. Energy*, Vol. 155, pp.484-499(2020).

Patterson, J.R., Cardiff, M., Feigl, K.L., “Optimizing geothermal production in fractured rock reservoirs under uncertainty,”; *Geothermics*, Vol. 88:101906(2020).

Pruess, K., “The TOUGH codes: A family of simulation tools for multiphase flow and transport processes in permeable media,”; *Vadose Zone J.*, Vol.3, pp.738-746(2004).

Ren, X., Zhou, L., Zhou, J., Lu, Z., Su, X., “Numerical analysis of heat extraction efficiency in a multilateral-well enhanced geothermal system considering hydraulic fracture propagation and configuration,”; *Geothermics*, Vol. 87: 101834(2020).

Wang, G., Song, X., Shi, Y., Yang, R., Yulong, F., Zheng, R., Li, J., “Heat extraction analysis of a novel multilateral-well coaxial closed-loop geothermal system,”; *Renew. Energy*, Vol. 163, pp. 974-986(2021).

Xu, T., Rose, P., Fayer, S., Pruess, K., “On modeling of chemical stimulation of an enhanced geothermal system using a high pH solution with chelating agent,”; *Geofluids*, Vol. 9, pp. 167-177(2009).

Xu, T., Sonnenthal, E., Spycher, N., Pruess, K., “TOUGHREACT: A simulation program for non-isothermal multiphase reactive geochemical transport in variably saturated geologic media,”;

Comput. Geosci., Vo. 32, pp. 145-165(2006).

地熱能之熱阻產能評估方法：清水地熱井IC09、IC13個案探討

林大偉 加娜朋

國立臺南大學機電系統工程研究所

摘要

因為我們對儲集層中的熱流現象所知太少，導致目前除了現地產能測試外並沒有有效的方法可以去預估地熱電廠的效能。本研究以地熱井總熱阻為概念提出了一個創新的產能測試評估方法。本研究將布林克曼孔隙流場模型、管流模型及孔隙熱傳模型耦合為一地熱產能評估模型。首先，本研究先利用清水地熱區之地熱井IC09及IC13之產能測試結果建立地熱井之熱阻值。繼而，藉由此熱阻值以掌握不同流量與溫度下之產能關係。此模型可以獲得一特定地熱井合理成本下之產能值，以進行地熱井發電之規劃。以熱阻之角度著手建立地熱井之效能為本研究所提出最關鍵之技術，可據此建立一可靠方便之產能評估工具。